Excitation of the isovector giant monopole resonances via the ^{nat}Pb(^{3}He,tp) reaction

R. G. T. Zegers,[1,*] A. M. van den Berg,[1] S. Brandenburg,[1] M. Fujiwara,[2,3] J. Guillot,[4] M. N. Harakeh,[1] H. Laurent,[4] S. Y. van der Werf,[1] A. Willis,[4] and H. W. Wilschut[1]

[1]*Kernfysisch Versneller Instituut, Zernikelaan 25, 9747 AA Groningen, The Netherlands*

[2]*Research Center for Nuclear Physics, Osaka University, Ibaraki, Osaka 567-0047, Japan*

[3]*Japan Atomic Energy Research Institute, Advanced Science Research Center, Tokai 319-1195, Japan*

[4]*Institut de Physique Nucléaire, IN2P3, Université de Paris-Sud, Orsay Cedex, France*

(Received 26 October 2000; published 20 February 2001)

The ^{nat}Pb(^{3}He,t) reaction and the subsequent decay of the excited nucleus by proton emission at backward angles were studied at $E(^3\mathrm{He}) = 177$ MeV with the aim to separate the $2\hbar\omega$ isovector monopole strength in Bi isotopes from the continuum background. Since the continuum is largely due to quasifree processes associated with forward-peaked high-energy protons, the observed resonance-to-continuum ratio is drastically improved when coincidences between ejectile tritons and protons emitted at backward angles are required. Furthermore, the cross section for the monopole resonances excited via (^{3}He,t) is, unlike the cross sections for higher multipolarity excitations, strongly forward peaked. By comparing coincidence spectra at $\theta_t \approx 0°$ and at finite angles, monopole strength was found in the region $-45 < Q < -30$ MeV. The measured monopole cross section is compared with distorted-wave Born approximation calculations for spin-flip and non-spin-flip isovector monopole excitations. It is found that 20% of the respective non-energy-weighted sum rules are exhausted in the proton-decay channel.

DOI: 10.1103/PhysRevC.63.034613 PACS number(s): 24.30.Cz, 25.55.Kr, 27.80.+w

I. INTRODUCTION

Isovector giant monopole resonances have been a subject of special interest for many years already [1]. They are classified as two different modes. The first one is the isovector non-spin-flip giant monopole resonance (IVGMR, $\Delta L = 0$, $\Delta S = 0$, $\Delta T = 1$) for which the excitation can be described macroscopically by compressional, out-of-phase breathing oscillations of protons and neutrons in the nucleus. The second one, the isovector spin-flip giant monopole resonance (IVSGMR, $\Delta L = 0$, $\Delta S = 1$, $\Delta T = 1$), is the spin-flip partner of the IVGMR. The IVSGMR is not so easily depicted in a macroscopic picture. However, from a microscopic point of view the two resonances are very similar. Both resonances are described as coherent superpositions of $2\hbar\omega$ one-particle–one-hole (1p-1h) transitions with a change in principal quantum number $\Delta N = 1$ and no change in orbital angular momentum ($\Delta L = 0$) [2,3].

The IVGMR and IVSGMR are of intrinsic interest because they represent fundamental modes of collective nuclear excitations induced by a compressive force and play an important role in understanding nuclear-structure and Coulomb effects. The IVGMR is thought to mediate isospin-symmetry breaking and isospin mixing via the long-range monopole term of the Coulomb interaction between the IVGMR and the isobaric analog state (IAS) [4,5]. On the other hand, experimental information about the IVGMR and IVSGMR is scarce. This is due to a combination of their large widths (~ 10 MeV) and the presence of a large non-resonant continuum background in the reaction spectra.

Until recently, evidence for the IVGMR was only found via $\Delta T_z = +1$ charge-exchange reactions: the (π^-, π^0) reaction on various targets [6–8] and the ^{60}Ni(^{7}Li,^{7}Be) reaction [9]. This can be understood since for $\Delta T_z = +1$ charge-exchange reactions the resonances have a lower excitation energy, their final states have only one isospin ($T = T_0 + 1$; T_0 is the isospin of the target ground state), and competing $1\hbar\omega$ resonances, such as the isovector giant dipole resonance (IVGDR, $\Delta L = 1$, $\Delta S = 0$) and the isovector spin-flip giant dipole resonance (IVSGDR, $\Delta L = 1$, $\Delta S = 1$, $\Delta J = 0,1,2$), are absent or at least strongly Pauli blocked. Still, the interpretation of the above-mentioned experimental results is seriously hampered because of the continuum background. Other attempts to locate the IVGMR, using the (π^+, π^0) [6–8], ^{90}Zr(n,p) [10], (^{13}C,^{13}N) [11–13], and ^{124}Sn(^{3}He,tn) [14] reactions, have been unsuccessful or at best ambiguous. Excitation of the IVSGMR was conjectured in the study of (^{3}He,t) singles spectra at projectile energies of 600 and 900 MeV [15,16] and the (p,n) reaction at 795 MeV [17]. Also, in these cases, the interpretation is ambiguous. Very recently, a comparative study of the ($\vec{p},\vec{n}$) reactions at 200 MeV and 800 MeV bombarding energies [18] gives an indication of the excitation of a strong resonance at forward scattering angles, suggesting the presence of the IVSGMR.

Since the early 1970s, various theoretical approaches have been developed to describe the IVGMR and IVSGMR. Transition matrix elements of the IVGMR were estimated by Auerbach in 1972 [19]. In 1975, calculations in a hydrodynamical framework were performed by Auerbach and Yeverechyahu [20]. In anticipation of the experimental results from the π-charge-exchange experiments, microscopic calculations for the IVGMR were performed [2,21,22]. Interpretation of the IVSGMR in terms of hydrodynamical calculations is complex because of the difficulty in treating the

*Present address: Japan Atomic Energy Research Institute, Advanced Science Research Center, Tokai 319-1195, Japan.

spin degree of freedom. Auerbach and Klein performed calculations for the IVSGMR in a Hartree-Fock, random-phase approximation (HF-RPA) framework [3] and concluded that the strength distributions for the IVGMR and IVSGMR are similar in location and shape. The relative contributions of the two resonances to the monopole cross section are determined by the energy dependence of the effective nucleon-nucleon (NN) interaction and the Q-value dependence of the reaction mechanism [23,24]. At bombarding energies $E \geqslant 100$ MeV/nucleon, isovector non-spin-flip transitions mediated through the V_τ component of the effective force are weak compared to contributions from spin-flip transitions, which are mediated through the $V_{\sigma\tau}$ and $V_{T\tau}$ components of the force. The opposite is true for $E \leqslant 50$ MeV/nucleon. Furthermore, at low bombarding energies the cross sections of the IVSGMR and IVGMR are expected to decrease strongly as a function of their excitation energy because of the increasing momentum mismatch (see also below). This article deals with the study of the $^{\text{nat}}$Pb(^{3}He,t) reaction at $E(^3\text{He}) = 177$ MeV. The basic results have previously been reported in Ref. [25]. The expected cross section for the IVGMR reaches a maximum at this bombarding energy, although it is still considerably lower than that expected for the IVSGMR.

In order to investigate the various giant resonances excited in charge-exchange reactions often a phenomenological description for the quasifree processes is employed to remove their contributions from the measured spectra. This method was introduced by Erell *et al.* [6] for the π-charge-exchange reaction. It can, however, lead to large systematic errors for the extracted giant-resonance cross sections and is not applicable to investigate the IVGMR and IVSGMR excited via the single-arm (^{3}He,t) reaction discussed in this paper. Therefore, an exclusive measurement was performed by requiring coincidences between the tritons at very forward angles, including zero degrees, and protons emitted at backward angles. In this way the relative contribution of the continuum background is strongly reduced. This method is based on the fact that the quasifree continuum is largely due to the breakup pickup (BU), i.e., breakup of the projectile and subsequent nucleon pickup from the target, and charge-exchange knockon (KO) reactions. Both processes are associated with forward-peaked high-energy protons in coincidence with the tritons [26,27]. In the plane-wave impulse approximation (PWIA), their cross sections are simply but realistically expressed as

$$\frac{d^2\sigma}{d\Omega_1 dE_1}(\text{BU}) = \text{phase space} \times |T_{2A}|^2 \left| \Phi\left(\vec{p}_1 - \frac{1}{3}\vec{p}_{[^3He]} \right) \right|^2, \tag{1}$$

$$\frac{d^2\sigma}{d\Omega_1 dE_1}(\text{KO}) = \text{phase space} \times |T_{1A}|^2 |\Phi(\vec{p}_1)|^2, \tag{2}$$

where particle 1 is the emitted proton. In BU, a proton inside the ^{3}He is a spectator and T_{2A} is the T matrix for quasifree single-neutron pickup leading to the outgoing triton. In KO the proton results from a quasifree $n(^3\text{He},t)p$ reaction. The factor $|\Phi|^2$ gives the momentum distribution of the spectator proton inside the projectile in BU and that of the struck neutron in KO. Both cross sections are forward peaked, in BU by the spectator momentum distribution and in KO by the properties of the quasifree T matrix. Since particle decay from monopole resonances, like the IVSGMR and IVGMR, is isotropic, the requirement of a coincidence between a forward triton and a proton emitted at backward angles strongly suppresses the contribution of the BU and KO processes to the continuum background and thus increases the resonance-to-continuum ratio.

Of course, the applicability of the method strongly depends on the branching ratios for proton decay from the resonances under investigation. Roughly speaking, decay from an excited nucleus can occur in two ways. The first one is direct decay (associated with the escape width, $\Gamma^\uparrow$), i.e., particle emission from the first step due to a strong overlap between the 1p-1h excited stated and the ground or single-hole state of the residual nucleus coupled to a particle in the continuum. This decay mode is, in the case of $\Delta T_z = -1$ excitations, strongly associated with proton decay, because the doorway states of the resonances have 1π(particle)-1ν(hole) structure (for $\Delta T_z = +1$ excitations, the situation is reversed and a neutron particle in the continuum and a proton-hole state is created, thus resulting in direct neutron emission).

The second decay mode is associated with decay from the so-called compound nucleus, i.e., after the excited state has coupled to more and more complex configurations (np-nh) and reached statistical equilibrium. Different decay channels will compete and emission will occur statistically (the resulting width is the so-called spreading width $\Gamma^\downarrow$). In the case of heavy nuclei, this decay channel is strongly dominated by neutron (and γ) emission, since the Coulomb barrier effectively inhibits statistical decay by proton emission. If statistical decay is dominant, then sufficiently high rates can be expected by investigating the neutron-decay channel. Along this line of thought an experiment was performed to measure the IVGMR and IVSGMR via the ^{124}Sn(^{3}He,tn) reaction [14], requiring coincidences between tritons at forward angles and neutrons at backward angles. However, no evidence for the presence of the IVGMR and IVSGMR was obtained.

It should also be noted that decay from an intermediate state in the equilibriation process (preequilibrium) also occurs.

Over the last decade, there has been growing evidence that doorway states of the giant resonances excited via the (^{3}He,t) reaction have nonvanishing escape widths for direct proton decay into low-lying neutron hole states. Total branching ratios for the direct proton decay channel for the Gamow-Teller resonance (GTR, $\Delta L = 0$, $\Delta S = 1$) of 4.9% $\pm$ 1.3% [28,29] and for the isovector spin-flip giant dipole resonance (IVSGDR) of 13.4% $\pm$ 3.9% [29,30] have been reported, both excited via the ^{208}Pb(^{3}He,t) reaction at 450 MeV. These results are well reproduced by calculations in an extended continuum RPA framework by Moukhai *et al.* [31]. Similar calculations predict a high proton branching ratio ($\geqslant 50\%$) for both the IVGMR and IVSGMR in ^{208}Bi [32]. This is due to two effects. First, for these resonances at an excitation energy of approximately 35 MeV, the available

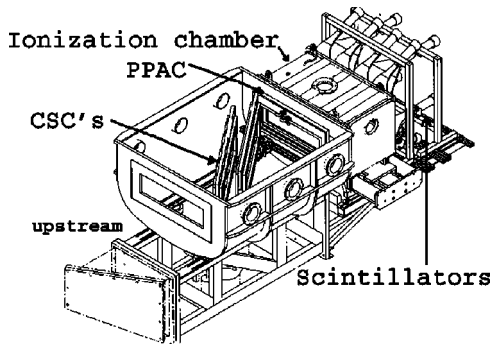

FIG. 1. The focal-plane detection system made by IPN Orsay which consists of the cathode-strip chambers (CSC's), scintillators, ionization chamber, and parallel-plate avalanche counter (PPAC) (the latter two were not used in the present experiment). The CSC's are placed inside a vacuum tank which is fitted to the exit of the dipole magnet of the BBS spectrometer.

kinetic energy for proton decay is large, thereby diminishing the importance of the Coulomb barrier. Second, the authors argue that the spreading width saturates at higher excitation energies. The branching ratio for direct proton decay thus increases with excitation energy, making it a useful probe to locate these resonances. Furthermore, investigating the branching ratios for direct proton decay of a giant resonance is of great interest, since the results serve as a quantitative test of the wave functions which result from microscopic theoretical calculations.

The expected nonvanishing branching ratios for decay by proton emission from the IVSGMR and IVGMR and the method of increasing the resonance-to-continuum ratio by requiring coincidences between the forward triton and backward emitted proton form the basis for the presently discussed experiment.

II. EXPERIMENTAL SETUP

A 177 MeV $^3He^{2+}$ beam was accelerated with the AGOR cyclotron at KVI and transported to Big-Bite Spectrometer (BBS) [33]. The target was a metallic foil of ^{nat}Pb with a thickness of 7.8 mg/cm^2 thickness. A focal-plane detection system constructed at IPN Orsay [34,35] (see Fig. 1) was used to detect the tritons. Two cathode-strip chambers (CSC's) put in the focal plane of the BBS to serve as position-sensitive detectors. Each CSC consists of five planes: a central cathode plane, two cathode-strip planes (one on each side of the central plane), and two anode-wire planes which are placed between the cathode-strip planes and the central cathode plane. The electron avalanche at the anode wires created through gas ionization by a passing particle induces an image charge on the cathode strips. These charge signals are preamplified and read out. The centroid of the charge distribution is calculated on-line by a digital-signal processor (DSP). For details on the electronics of the detection system, see Ref. [36]. Each of the CSC's has so-called ''*U*-type'' and ''*V*-type'' planes; i.e., their strips are at right angles with each other and at 45° with the horizontal plane. From the *U* and *V* coordinates found in each of the CSC's, horizontal and vertical positions in the detectors can be calculated and by combining the results of the two CSC's the horizontal and vertical angles can be determined. The cathodes consist of 128 gold strips with a width of 6 mm and a pitch of 6.4 mm. The anodes consist of gold-plated tungsten wires with a diameter of 20 μm and with a pitch of 3.2 mm. The central cathode decouples the *U* and *V* parts of the chamber and the electric field in each part is shaped by the anode plane and two cathode planes. The distance between each of the anodes and the central cathode is 8 mm and the distance of the anodes to the stripped cathodes is 6 mm. The total surface of the detection area is 974×250 mm^2. The detector gas used was an argon-ethane mixture (80%/20%) and was kept at a pressure of 1 bar. The CSC's are placed inside a vacuum tank. At the exit of the tank a 1 mm thick stainless steel plate was mounted which enables the particles to reach a segmented scintillator stack that is mounted behind the vacuum tank. The first layer of scintillators has four segments of 2 mm thickness each and the second layer has two segments of 5 mm thickness each. The stack serves different purposes. It provides the event trigger, gives the stop signal for the time-of-flight (TOF) measurement with respect to the rf of the cyclotron of particles passing through the spectrometer, and is used for particle identification and exclusion of experimental background by means of ΔE-E measurements.

The BBS consists of two quadrupole magnets and a dipole magnet. The two quadrupole magnets are located upstream from the dipole magnet and the distance with respect to the dipole magnet can be varied to change the optical properties of the spectrometer. For this experiment, mode B (for details, see Ref. [33]) was used. In this mode, the BBS has a large maximum solid angle (9.2 msr, i.e., a maximum horizontal opening angle of 66 mrad and a maximum vertical opening angle of 140 mrad), which allows one to cover a large angular range in one setting. The opening angle of the BBS was set to center around $-1°$ with respect to the beam; i.e., the beam entered the spectrometer off center, along the concave (shorter-radius) edge of the dipole. The beam was stopped in a Faraday cup which was placed inside the dipole magnet. The beam current (~1 *e* nA) was read out for absolute cross-section determination. Careful tuning of the beam could not prevent some scattering in the Faraday cup to be present in the measured data. However, since the cup was shielded from the detectors used for measuring decay protons from the target at backwards angles (see below), this background can only contribute to random coincidences between tritons in the focal plane and decay protons.

Relevant experimental observables (i.e., the scattering angle and momentum of the scattered particle) are found by tracing measured quantities in the focal plane back to the target. The parameters needed to perform this ray tracing are deduced from a calibration measurement using a ''sieve slit'' which is placed in front of the opening of the spectrometer (for the procedure, see [37]). Although such a calibration was performed during this experiment, a special angle-defining aperture was used to make hardware cuts in the solid angle of the BBS. This aperture is displayed in Fig. 2. There are three rectangular holes, centered at vertical scat-

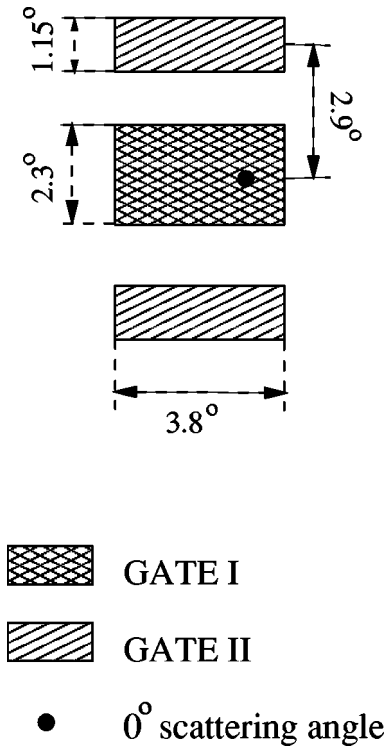

FIG. 2. The angle-defining aperture used to obtain very accurately defined cuts in the opening angle of the spectrometer (see text).

tering angles of $-2.9°$, $0°$, and $+2.9°$, with vertical opening angles of 1.15°, 2.3°, and 1.15°, respectively. The horizontal opening angle was 3.8° and thus triton scattering angles between 0° and ~4.7° were covered. The central hole in the aperture encompasses the maximum (0°) of the angular distributions of the IVSGMR and IVGMR (see below) and will be referred to as ''gate I'' throughout this article. The average scattering angle in gate I is 1.4°. The upper and lower holes encompass the first minimum in the angular distributions of the IVGMR and IVSGMR (~3°) and the combination of the two is called ''gate II.'' The average triton scattering angle for this gate is 3.2°. Using these gates, very clean cuts in scattering angle are obtained.

Although the momentum bite of the BBS is large (19%), the momentum range was limited by the focal-plane detection system and the need to reduce experimental background. A Q-value range of 33 MeV could be covered. It was decided to measure the range between $Q=-15$ MeV and $Q=-48$ MeV, since besides covering the range of interest for the IVGMR and IVSGMR (expected at $Q\sim-38$ MeV with a width of ~10 MeV), also the IAS ($Q=-18.1$ MeV) will be included in the spectra, which is convenient for calibration purposes and comparison with previous experimental results. Matters are complicated by a seriously degraded resolution of the vertical scattering angle when the BBS is tuned to give point-to-point focusing from target to focal plane. This is due to the fact that the vertical position in the focal plane is the main parameter for determining the vertical component of the scattering angle and, as explained above, this information is crucial for the experiment. The problem

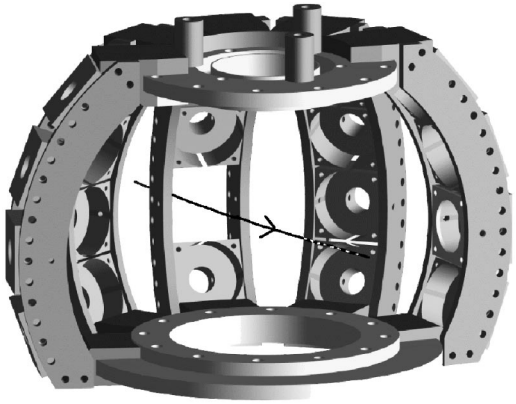

FIG. 3. The Silicon-Ball charged-particle detector as used in the ^{nat}Pb(^{3}He,tp) experiment at KVI. The detectors themselves are not shown. One position is left open for the beam (as indicated by the arrow) to pass through. Generally speaking, the position and number of detectors are adjustable to match demands for specific experiments.

can be solved by increasing the magnetic fields of the first quadrupole magnet to move the vertical focal plane upstream and approach point-to-parallel focusing. For the BBS in mode B, applicability of this method is restricted by the loss in vertical acceptance and the method only works for part of the momentum bite. The Q-value range where good vertical-position resolution in the focal plane and thus good resolution for the vertical component of the scattering angle can be obtained was chosen to be between $Q=-27$ MeV and $Q=-48$ MeV. This is, of course, the range of interest for the IVGMR and IVSGMR. The energy resolution obtained was 360 keV. The energy resolution of the spectrometer and the incoming beam contributes 250 keV to this number. The remainder is due to the difference in energy loss in the target for tritons and ^{3}He, respectively.

Protons were detected in the so-called ''Silicon Ball'' [37]. For the present experiment it consisted of 15 lithium-drifted silicon [Si(Li)] detectors, each of which has a thickness of 5 mm and an effective area of 450 mm^2. A drawing of the configuration used is shown in Fig. 3. Fifteen detectors were placed at polar angles ranging from 95° to 160° and azimuthal angles between $-20°$ and 40°, each at a distance of 10 cm from the target. One position, in the central arm, was left open to allow the beam to pass through. Almost 6% of the full solid angle was covered. The detectors were cooled through conduction by liquid alcohol to a temperature of $-30\,°$C to improve the resolution to a typical value of 30 keV [38]. Because of the limited thickness of the Si(Li) detectors, protons with an energy higher than 30 MeV will punch through and consequently deposit less than their full energy (see Fig. 4). This results in an ambiguity in the determination of proton energy for decay from highly excited states in the present experiment and it is, therefore, difficult to distinguish between the various decay modes (direct, statistical, or semidirect) as will become clear in the discussion of the results below. In the experiment, it was not necessary to perform particle identification [by means of putting ΔE detectors in front of the Si(Li) detectors] for particles emitted

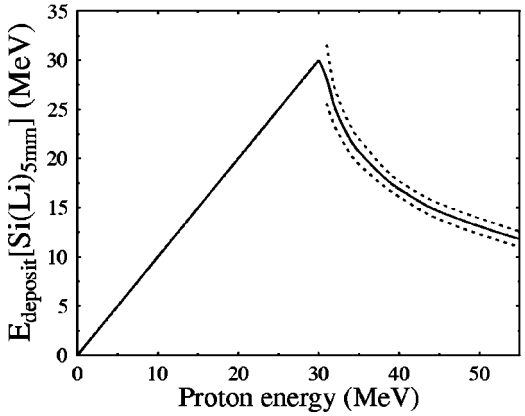

FIG. 4. The energy deposited in 5 mm thick Si(Li) detectors as a function of proton energy. At a proton energy of approximately 30 MeV the protons punch through the detector and deposit less energy. The dotted lines indicate the uncertainty due to straggling (note that the intrinsic detector resolution is only 30 keV).

at backward angles. Decay by α-particle emission is, as a consequence of the Coulomb barrier, strongly inhibited and can be neglected. ^{3}He particles due to elastic scattering from the target and deuterons from breakup processes are strongly forward peaked and, moreover, only contribute to random coincidences. The prompt-to-random coincidence ratio was approximately 3 to 1.

During the experiment, singles and coincidence data were taken simultaneously. The former were downscaled by a factor of 16. The focal-plane detection efficiency was 98%, determined by comparing the accepted events with the number of triggers from the scintillator detectors. The electronics live time was 99%.

III. SINGLES DATA

In Fig. 5 the singles Q, value spectrum is shown. The Q values for the excitation of the IAS in Bi for the various isotopes in ^{nat}Pb (52.3% ^{208}Pb, 22.6% ^{207}Pb, 23.6% ^{206}Pb,

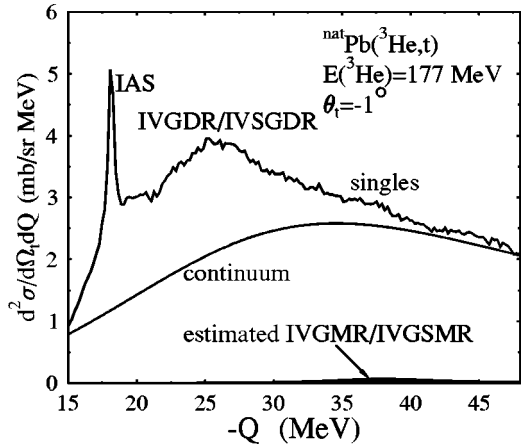

FIG. 5. Singles Q-value spectrum for the ^{nat}Pb(^{3}He,t) reaction at 177 MeV and $\theta_t = -1°$. A phenomenological approximation for the continuum background (see text) as well as the estimated contribution to the spectra from the IVGMR and IVSGMR is drawn.

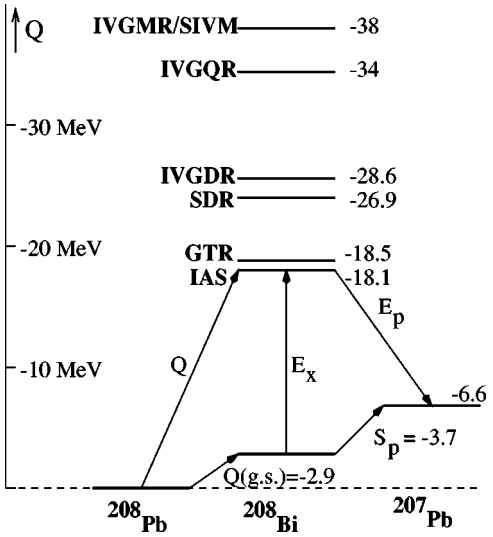

FIG. 6. Level scheme indicating the various giant resonances excited via the ^{208}Pb(^{3}He,t) reaction and their subsequent decay by proton emission.

and 1.5% ^{204}Pb) are similar (-18.06 MeV, -18.12 MeV, -18.16 MeV, and -18.27 MeV [39], respectively) since they essentially depend on the Coulomb displacement. With the resolution of 360 keV, they cannot be distinguished and the IAS's were observed as one single peak. The large bump in Fig. 5 at $Q \sim 25$ MeV is due to the IVGDR and IVSGDR; the GTR is situated between the IAS and this bump, but can hardly be distinguished. An estimate of the continuum background is drawn in the figure based on the phenomenological description by Errell *et al.* [6]. Estimates for the parameters used are very similar or equal to the ones used in Ref. [40]. An estimate for the combined cross section due to the IVGMR and IVSGMR is also shown (the cross-section calculations are discussed below), situated at and assumed $Q = -38$ MeV and a width of 10 MeV. As can be seen, it only accounts for a small fraction of the total cross section contained in the continuum and, with the uncertainty in the description of the quasifree continuum and possible contaminations due to experimental background, it is impossible to draw any conclusions on its existence from such a singles spectrum.

Figure 6 shows a level scheme for the various resonances excited via the ^{208}Pb(^{3}He,t) reaction. The positions of the resonances are expected to be very similar for the various Pb isotopes. Note that the Q values for the decay by proton emission from the relevant Pb isotopes are equal within 0.5 MeV. The Q value for the IVGMR was calculated using [41]

$$Q^{IVGMR} = Q^{IAS} - V_0 A^{-1/3} - (T_0 + 1) V_1 / A, \qquad (3)$$

where V_0 and V_1 depend on the model used. It is assumed that only the lowest of the three possible isospin components of the IVGMR is excited. This is to a large extent true for heavy nuclei with large neutron excess [in the case of ^{208}Pb more than 95% of the transition probability should go to this component, as estimated from the isospin-coupling (Clebsch-Gordan) coefficients]. In the hydrodynamical model V_0

equals 170 MeV [41] but other approaches [2] suggest a lower value of 155 MeV. V_1 has been found to be strongly quenched with respect to the single-particle symmetry potential ($\approx$100 MeV [41]) and is approximately 60 MeV [2,20,42,43]. We thus find a rough estimate of -38 MeV for the Q value of the IVGMR in ^{208}Bi. For the width of the IVGMR the situation is very unclear. Predictions vary between 5 and 15 MeV [2,5,6,20]. The Q value for the IVSGMR is assumed to be equal to that of the IVGMR. For the isovector giant quadrupole resonance (IVGQR) V_0 was taken 130 MeV [1]. The positions of the GTR and IVSGDR were taken from Refs. [28–30] and the position of the IVGDR is taken from Ref. [44].

Calculations in the distorted-wave Born approximation (DWBA) framework were performed to estimate the cross sections of the IVGMR and IVSGMR excited through the ^{208}Pb(^{3}He,t)^{208}Bi reaction. To this end, wave functions projected on a complete 1p-1h basis were calculated in a normal-mode procedure [41,45]. In this approach, the response of the nucleus to the action of an operator O is expanded over the 1p-1h basis:

$$|\mathrm{NM}_{T,LSJM}\rangle = N^{-1}\sum_{ph} v_{j_h}u_{j_p}|j_p,j_h^{-1};JM\rangle \times\langle j_p j_h^{-1};JM||O_{T,LSJ}||0\rangle. \quad (4)$$

For isovector non-spin-flip modes the operator is

$$O_{T=1,L0J} = r^{\lambda}Y_L t_z, \quad (5)$$

where λ usually equals the multipolarity L except for the IVGMR, in which case $\lambda=2$, and t_z is the third component of the isospin operator. The ground-state neutron-hole occupation probabilities, represented by the fullness parameter $v^2(j)$, and the proton-particle occupation probabilities, represented by the emptiness parameter $u^2(j)$, were chosen as unity and zero, respectively, since ^{208}Pb is a doubly magic nucleus. Generally speaking, $v_j^2+u_j^2=1$ holds for all j. For isovector spin-flip modes the operator is

$$O_{T=1,L1J} = r^{\lambda}[\sigma\otimes Y_L]_J t_z. \quad (6)$$

Similar to the non-spin-flip case, λ usually equals L, except for the IVSGMR, in which case $\lambda=2$.

The factor N in Eq. (4) is chosen such that the normal mode exhausts the full multipole strength:

$$S_{TLJ} = \sum_M |\langle \mathrm{NM}_{T,LSJM}|O_{T,LSJ}|0\rangle|^2 = \sum_{ph} v_{j_h}^2 u_{j_p}^2 |\langle j_p,j_h^{-1};JM||O_{T,LSJ}||0\rangle|^2. \quad (7)$$

In other words, 100% of the non-energy-weighted sum rule (NEWSR) associated with the operator $O_{T,LSJ}$ is exhausted. For the IVGMR and IVSGMR, which are $2\hbar\omega$, $J^\pi=0^+$ and 1^+ transitions, respectively, many p-h configurations contribute. Calculations were performed using the code NORMOD [46]. The strengths calculated for the IVGMR, IVSGMR, and also the IAS and GTR are listed in Table I.

TABLE I. Transition strengths calculated in a normal-mode procedure (see text).

Mode	Strength
IAS	3.5
GTR	10.5
IVGMR	2229 fm^4
IVSGMR	6146 fm^4

The value found for the strength of the IAS, when multiplied by 4π [because of the presence of Y_L with $L=0$ in the operator definition (4)], equals 44, which is the Fermi sum rule $(N-Z)$ for ^{208}Pb. Likewise, if the value found for the GTR is multiplied by 4π, the Ikeda-Fujii-Fujita sum rule $3(N-Z)$ is found. The values for the IVGMR and IVSGMR are larger than the results from the HF-RPA calculations by Auerbach and Klein [2,3] by a factor of 2–3. Note that the definition for the monopole operator used by these authors differs by a factor $\sqrt{8\pi}$ from Eq. (5). If this is taken into account, their numbers for the strength of the IVGMR and IVSGMR, 2.5×10^4 fm^4 and 4.5×10^4 fm^4, respectively, become 1000 fm^4 and 1776 fm^4. The reason for this overestimation is similar to the difference between HF-RPA and Tamm-Dancoff (TD) calculations [3], namely, that the HF-RPA approach takes ground-state correlations into account, in contrast to the TD and normal-mode calculations.

DWBA calculations were performed using the code DW81 [47]. An effective projectile-target interaction was used where the interaction is written in terms of Yukawa functions (for an extensive discussion see [24,48]). Parameters for the interaction were taken from the preliminary analysis of the ^{12,13,14}C(^{3}He,t)^{12,13,14}N reactions at 200 MeV [49] and from the ^{40}Ca(^{3}He,t)^{40}Sc($2_1^-+5_1^-$) reaction at 197 MeV [50], except for the central isospin strength (V_τ) which was determined from fitting the cross section of the IAS to the calculation. A value for V_τ of 3.5 ± 0.1 MeV was found (see below), corresponding well to previously extracted values from (^{3}He,t) experiments at a similar bombarding energy [37,40]. The other parameters were taken: $V_{\sigma\tau}=-3.5$ MeV, $V_{T\tau}=-3.0$ MeV, while $V_{LS\tau}$ was kept zero [24]. The ^{3}He optical-model parameters were taken from the literature (^{3}He on ^{208}Pb at 217 MeV [51]). For the tritons the potential-well depths were taken 85% of the depths for the ^{3}He particles [52].

Results for transitions with $\Delta L=0$ (top panel), 1 (center panel), and 2 (bottom panel) are displayed in Fig. 7. In addition to the IVGMR and IVSGMR, these include the results for the IAS, GTR, IVGDR, IVSGDR (components with $J^\pi=0^-,1^-$, and 2^- at $E_x=23.8$ MeV, $E_x=22.9$ MeV, and $E_x=20.1$ MeV, respectively [53]), and IVGQR. The appropriate normal-mode wave functions for each resonance were used. The monopole transitions peak at 0° and have a minimum around 3°. The IVSGMR is dominant over the IVGMR by more than a factor of 3. The summed cross section of the IVSGMR and IVGMR at 0° is almost 30% of that for the IAS.

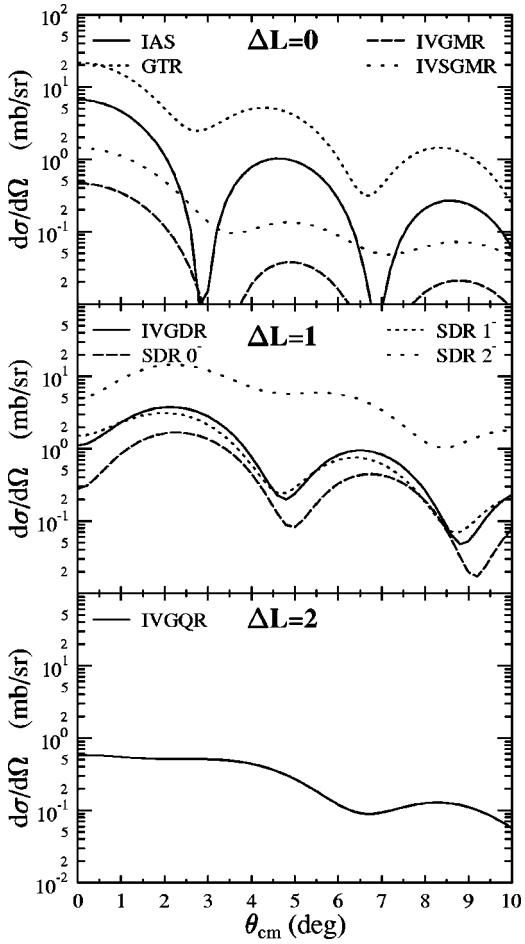

FIG. 7. DWBA calculations for the monopole (top panel), dipole (center panel), and quadrupole (bottom panel) isovector giant resonances excited via the ^{208}Pb(^{3}He,t) reaction at 177 MeV.

Figure 7 shows that the dipole resonances peak around 2.5°. The 2^- component of the IVSGDR is dominant. The IVGQR is more or less flat below 4°. Its cross section at 0° is larger than that of the IVGMR but lower than that of the IVSGMR. Since the IVGQR is also expected to have a rather large width, it overlaps with the IVSGMR and IVGMR. Therefore, these resonances can only be distinguished by comparing spectra at different scattering angles.

As a result of the fact that there was some experimental background present in the singles data which could not be taken away by applying software cuts in the off-line analysis, only the angular distribution of the IAS was carefully investigated, since it is such a well-defined peak. The DW81 calculations were transformed to the laboratory frame and folded according to the angular apertures subdivided into six 11 mrad wide bins. The comparison between the calculations and experimental results are shown in Fig. 8, showing excellent agreement.

IV. COINCIDENCE DATA

Figure 9 shows the coincidence Q-value spectrum. Its basic structure is similar to that of the singles spectrum; a strong peak due to the IAS and a bump at $Q\sim25$ MeV are seen. The branching ratio for proton decay from the IAS in Bi was determined to be $69\%\pm3\%$, which is consistent with the result of $64\%\pm4\%$ obtained by weighting previously measured branching ratios of the IAS for the various targets of Pb isotopes ($73\%\pm14\%$ for ^{204}Pb, $60.5\%\pm4.2\%$ for ^{206}Pb, $67.7\%\pm4.5\%$ for ^{207}Pb [39], and $63.5\%\pm3.0\%$ for ^{208}Pb [54]) with the isotopic natural abundances. This high branching ratio, which is associated with direct decay, is due to the fact that decay from the IAS by (statistical) neutron emission is isospin forbidden and is only possible as a result of isospin mixing. Since the IAS is located above the Coulomb barrier, proton decay is allowed.

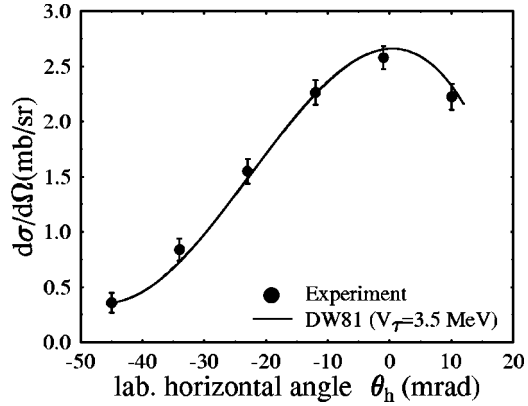

FIG. 8. Differential cross section of the IAS as a function of the laboratory horizontal angle and fitted DWBA calculation. The calculated curve is folded over 11 mrad wide bins to compare with the data.

Caution is needed to interpret the bump at $Q\sim25$ MeV. In first instance, one would associate it with proton decay from the IVGDR and IVSGDR. It can be shown using the PWIA of Eq. (2) [37,55,56], however, that contributions from charge-exchange KO to the coincidence spectra also peak around this Q value. In both the direct-decay process from the IVGDR/IVSGDR and the KO process, the same neutron-hole residual states are populated and the two cannot be separated experimentally. It was also found that the proton detectors positioned at the most forward angles (θ_p

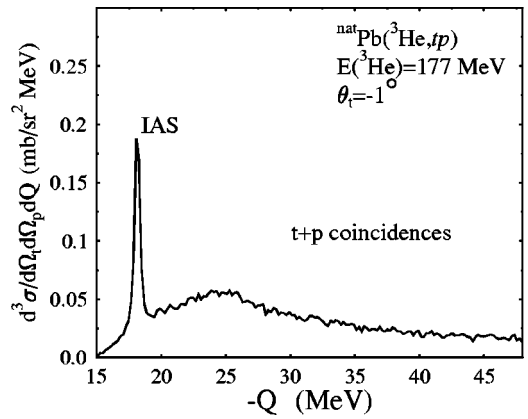

FIG. 9. Coincidence Q-value spectrum for the $^{\text{nat}}$Pb(^{3}He,tp) reaction at 177 MeV and $\theta_t=-1°$.

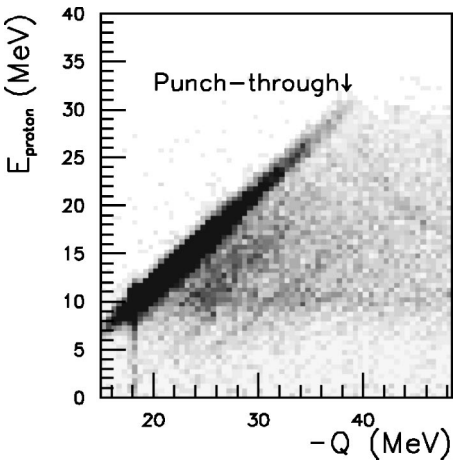

FIG. 10. Proton energy versus Q for the ^{nat}Pb(^{3}He,tp) reaction at 177 MeV. The point where high-energy protons punch through the 5 mm thick Si(Li) detectors is indicated (see Fig. 4).

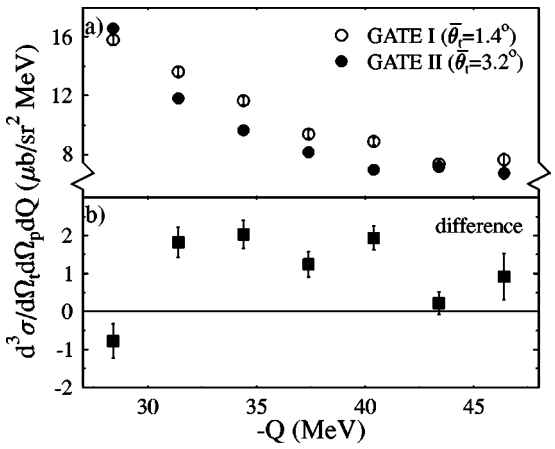

FIG. 11. (a) Coincidence spectra for the ^{nat}Pb(^{3}He,tp) reaction at 177 MeV for $\bar{\theta}_t$=1.4° (GATE I) and $\bar{\theta}_t$=3.2° (GATE II). (b) The difference between the spectra in (a).

=95°) had significantly (factor of 2) more events than the proton detectors at more backward angles. This is possibly another indication for KO or BU components in the coincident spectra. It must be realized, however, that decay from the IVGDR and IVSGDR is also not isotropic and that it is, therefore, impossible to draw conclusions on the nature of the bump at $Q\sim 25$ MeV using these experimental results. Better insight can only be gained by studying the coincidences between tritons and protons emitted at much more forward angles where BU and KO processes are dominant, but this was not pursued in the present experiment. For the analysis of the Q value range of interest for the IVGMR and IVSGMR, the proton detectors put at the most forward angles were excluded, as a result of the suspected high contibutions form KO or BU.

In Fig. 10, the proton energy is plotted versus Q value. The punch-through point ($Q\approx -38$ MeV), i.e., the point at which protons have sufficient energy to pass through the Si(Li) detector (see Fig. 4), is indicated. The dark diagonal band in Fig. 10 corresponds to a combination of decay from the excited nuclei to low-lying neutron-hole states (direct decay) and BU and KO processes. At Q values below -38 MeV, a very weak punch-through band can be distinguished (see Fig. 4). Protons emitted from the excited nucleus in a statistical way are expected to have an energy of approximately 10 MeV and to make up 0.1% of the total statistical decay according to calculations with the code CASCADE [57]. Although protons of ~ 10 MeV are detected, it is impossible to assign them to a certain decay process.

In order to investigate the possible presence of monopole strength, the (^{3}He,tp) spectra at different triton scattering angles were compared. The gates set by the angle-defining aperture (Fig. 2) were used. The result is shown in Fig. 11. The top panel shows the Q-value spectra for GATE I and GATE II and the bottom panel is the difference between the two. There is clearly an excess cross section in GATE I, i.e., forward scattering angles, which is a signature of monopole contributions to the spectra. The total excess in cross section in GATE I with respect to GATE II is 24 ± 2.8 μb/sr^2. The data points in the highest Q-value bin (45–48 MeV) have slightly larger error bars since a fraction of the opening angle below the median was cut due to a missing strip in the focal-plane detector and only events with a positive vertical scattering angle were used.

The angular correlation of the excess in cross section at forward triton scattering angles as a function of proton angle is plotted in Fig. 12. To make these figures, detectors with (nearly) the same polar angle [Fig. 12(a)] and azimuthal angle [Fig. 12(b)] are grouped together. The angular correlation is consistent with isotropy, as is expected for decay from monopole resonances. It is certainly not forward peaked and, therefore, these events are not due to KO or BU. We conclude that monopole strength has been found. For the determination of the exhaustion of sum-rule strength of the IVSGMR and IVGMR, the measured excess cross section is integrated over the full proton solid angle, with a result of 301 ± 35 μb/sr.

V. INTERPRETATION AND CONCLUSIONS

In order to determine the exhaustion of the NEWSR for the IVGMR and the IVSGMR, the experimental results have to be compared with the DWBA calculations. For the latter,

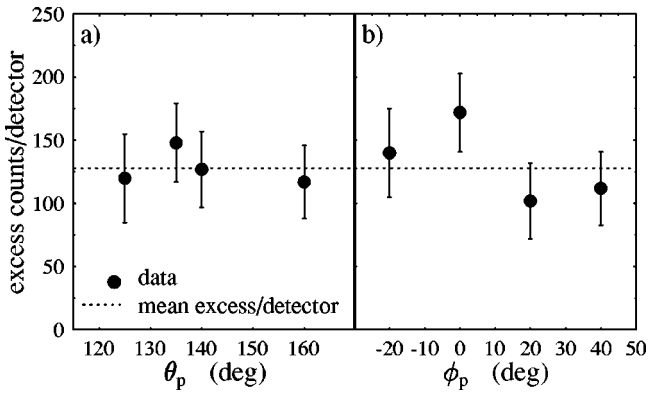

FIG. 12. Excess in counts at forward triton scattering angles (see Fig. 11) per proton detector as a function of θ_p (a) and ϕ_p (b). The dotted line is the average excess in counts per detector.

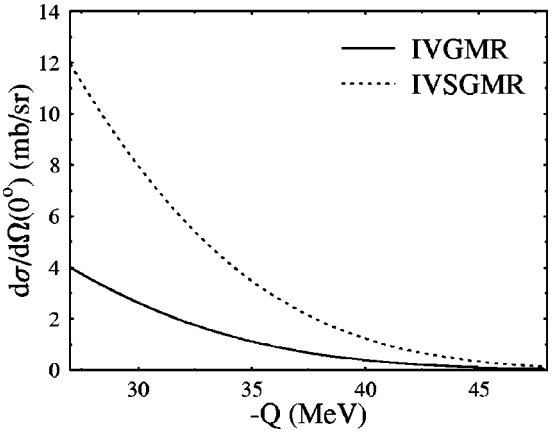

FIG. 13. Dependence of 0° cross sections of the IVGMR and IVSGMR on *Q*.

by definition the full NEWSR is exhausted because the normal-mode procedure was used to create the wave functions. Because of the large widths of the IVGMR and IVSGMR, cross-section calculations were performed for the full *Q*-value range of interest. The result is shown in Fig. 13. The cross section drops strongly per unit strength as a function of $-Q$. This is because of the increasing momentum transfer with decreasing *Q* and the fact that the monopole cross sections peak at zero momentum transfer. Although the IVSGMR is dominant by a factor of 3 over the IVGMR, contributions from the latter are not negligible. Since their angular distributions are so similar, it is impossible to distinguish between the monopole resonances from the present data.

The DWBA cross sections were folded over the opening angle defined by the special aperture and the experimental results were divided by these folded calculations. The exhaustion of the NEWSR for the IVGMR and IVSGMR as a function of *Q* value is shown in Fig. 14. The strength distribution peaks at $Q \approx -41$ MeV. The result of the highest *Q*-value bin (45–48 MeV) is not included in Fig. 14, because of the large error bar. The percentage of exhaustion in this bin is $20\% \pm 15\%$, which indicates that more monopole strength could be present beyond the range presently covered. Between $Q=-30$ MeV and $Q=-45$ MeV a fraction

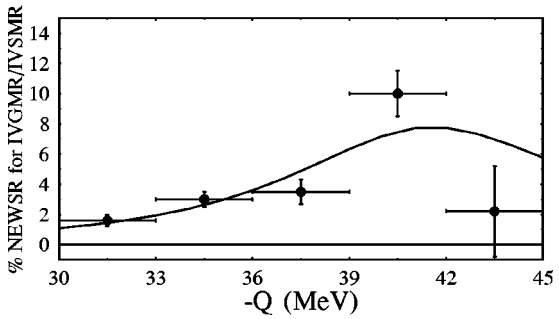

FIG. 14. Strength distribution extracted from the experimental results in terms of exhaustion of the NEWSR for the IVGMR and IVSGMR as a function of *Q*. The curve is the result of a fit with a Lorentzian (reduced $\chi^2=3$). Its width (Γ) is 11 MeV.

of 0.20 ± 0.04 of the NEWSR is found in the proton-decay channel. The curve in Fig. 14 is the result of a fit with a Lorentzian. Although the fit is poor, the extracted width (Γ) of 11 MeV is comparable with the predictions. The exhausted fraction of the NEWSR in the proton-decay channel indicates that if the branching ratio for decay by proton emission is 20%, the full NEWSR for the IVGMR and IVSGMR can be accounted for. If the calculation of the NEWSR in the normal-mode framework is indeed a factor of 2–3 too high, as suggested by the HF-RPA calculations, the branching ratio for proton emission from the IVSGMR and IVGMR should be higher by the same factor (if a linear relationship between strength and cross section is assumed) in order to not to exceed full exhaustion of the NEWSR.

As a result of the punch-through effect, it is impossible to distinguish between the various decay channels (i.e., statistical, direct, or an intermediate channel). However, an upper limit for the direct decay to the neutron-hole states below an excitation energy of 5 MeV in the residual nuclei was determined, by assuming that all events that have a measured proton energy corresponding to a punch-through proton belonging to such a decay, stem from direct decay only. It was found that $40\% \pm 20\%$ of the total ''monopole events'' are possible candidates for direct decay to these low-lying neutron-hole states, which corresponds to $8\% \pm 4\%$ of the normal-mode NEWSR. Since the statistical decay is very unlikely, the results suggest that a large fraction of the proton-decay channel goes through semidirect channels or direct channels to highly excited (deeply bound) neutron-hole states.

So far, we have assumed that the IVGMR and IVSGMR are superimposed on a ''background'' that has a flat angular distribution. Possible interference from other resonances was neglected. Although this is justifiable for the IVGQR, since it has a flat angular distribution, the tails of the IVGDR and IVSGDR distributions could influence the results. Also the possibility of high-lying Gamow-Teller strength cannot be ignored. The latter is a related to the fact that only 60% of the Ikeda-Fujii-Fujita sum rule is recovered in the main peak of the GTR [58]. It has been argued that this is caused by mixing of the 1p-1h states with 2p-2h states via the strong tensor interaction [59–61] which would result in shifting of Gamow-Teller strength to excitation energies up to 50 MeV. The other possible explanation is an admixture of the $\Delta(1232)$-isobar nucleon-hole (Δ-h) into the 1p-1h Gamow-Teller state [62] leading to a shift of Gamow-Teller strength would be shifted to excitation energies of ~ 300 MeV. In this latter case, no contributions in the excitation-energy range of importance for the IVGMR and IVSGMR is to be expected.

Influence from the tails of the dipole resonances was investigated by applying cuts in the opening angle different from the hardware cuts defined by the aperture, using the ray-tracing capabilities for the BBS. Since the monopole and dipole angular distributions are rather different, a possible interference between the two can be made visible by comparing spectra gated on different portions of the opening angle. It was found that a best fit to all cuts could be made if a small dipole contribution is assumed at high excitation en-

ergies. This would mean that the actual monopole cross section should be slightly larger than the value mentioned above (the monopole cross section integrated over the full proton solid angle would rise by 20% to 360 μb/sr).

Influence due to high-lying Gamow-Teller strength can only be investigated by comparing calculated strengths and cross sections, since the angular distribution of the GTR is very similar to those of the IVSGMR and IVGMR (see Fig. 7). As a test, we assumed that all monopole cross sections found are in fact due to high-lying Gamow-Teller strength. In that case, 52% of the Ikeda-Fujii-Fujita sum rule is exhausted in the proton-decay channel only. This is already more than the Gamow-Teller strength missing at lower excitation energies. Since the branching ratio for decay by proton emission is significantly smaller than 1, we conclude that the observed monopole cross section at high excitation energies can only for a minor fraction be due to Gamow-Teller strength. In fact, if we assume that all missing Gamow-Teller strength is indeed located in $-30<Q<-45$ MeV and, furthermore, that proton decay branching ratio for the IVGMR, IVSGMR, and GTR are equal, the DWBA calculations predict that 15% of the measured monopole cross section is due to Gamow-Teller strength. Therefore, the cross section assigned to the IVGMR and IVSGMR could be overestimated by 15% (i.e., the measured cross section due to the IVGMR and IVSGMR would drop to 256 μb/sr).

In conclusion, the present measurement of the ^{nat}Pb(^{3}He,$t+p$) reaction at $E(^3\mathrm{He})=177$ MeV revealed, for the first time, $2\hbar\omega$ isovector monopole strength in the $\Delta T_z=-1$ channel. We find that the measured monopole cross section for $-30<Q<-45$ MeV in the proton-decay channel is $301\pm35\pm60$ μb/sr, where the first error margin is of statistical and the second is of systematic nature. This strength is ascribed to the IVGMR and IVSGMR, and in terms of their NEWSR, $20\%\pm4\%\pm4\%$ is exhausted (note that the systematic error margin is determined under the assumption that the magnitude of interference due to dipole or Gamow-Teller strength is independent of Q value). Thus, if the branching ratio for proton emission from the IVGMR and IVSGMR is 20%, the full sum rules would be exhausted. Taking into account that the strengths calculated in the normal-mode procedure could well overestimate the true strengths by a factor of 2–3 (as indicated by HF-RPA calculations) the branching ratios should be higher. Such a high number is favored by recent calculations for the branching ratio for direct decay by proton emission from the IVSGMR and IVGMR in an extended continuum RPA framework ($\geqslant 50\%$) [31,32]. However, in the present experimental results it is impossible to separate the decay into different (i.e., statistical, direct, and semidirect) channels. Nevertheless, the upper limit for direct decay into neutron-hole states below an excitation energy of 5 MeV in the residual nucleus only amounts to $40\%\pm20\%$ of the total decay by proton emission from the IVGMR and IVSGMR, which corresponds to only $8\%\pm4\%$ exhaustion of the NEWSR. A branching ratio of $\geqslant 50\%$ for direct proton decay seems therefore unlikely.

ACKNOWLEDGMENTS

The authors wish to thank the cyclotron crew and staff at KVI for their support. The research was performed as part of the research program of the ''Stichting voor Fundamenteel Onderzoek der Materie'' (FOM) with financial support from the ''Nederlandse Organisatie voor Wetenschappelijk Onderzoek'' (NWO).

[1] See, for example, in *Electric and Magnetic Giant Resonances in Nuclei*, International Review of Nuclear Physics, Vol. 7, edited by J. Speth (World Scientific, Singapore, 1991).

[2] N. Auerbach and A. Klein, Nucl. Phys. **A395**, 77 (1983), and references therein.

[3] N. Auerbach and A. Klein, Phys. Rev. C **30**, 1032 (1984), and references therein.

[4] T. Suzuki, H. Sagawa, and G. Colò, Phys. Rev. C **54**, 2954 (1996), and references therein.

[5] J. Jänecke, M.N. Harakeh, and S.Y. van der Werf, Nucl. Phys. **A463**, 571 (1987), and references therein.

[6] A. Erell, J. Alster, J. Lichtenstadt, M.A. Moinester, J.D. Bowman, M.D. Cooper, F. Irom, H.S. Matis, E. Piasetzky, and U. Sennhauser, Phys. Rev. C **34**, 1822 (1986).

[7] A. Erell, J. Alster, J. Lichtenstadt, M.A. Moinester, J.D. Bowman, M.D. Cooper, F. Irom, H.S. Matis, E. Piasetzky, U. Sennhauser, and A. Ingram, Phys. Rev. Lett. **52**, 2134 (1984).

[8] F. Irom, J.D. Bowman, G.O. Bolme, E. Piasetzky, U. Sennhauser, J. Alster, J. Lichtenstadt, M.A. Moinester, J.N. Knudson, S.H. Rokni, and E.R. Siciliano, Phys. Rev. C **34**, 2231 (1986).

[9] S. Nakayama, H. Akimune, Y. Arimoto, I. Daito, H. Fujimura, Y. Fujita, M. Fujiwara, K. Fushimi, H. Kohri, N. Koori, K. Takahisa, T. Takeuchi, A. Tamii, M. Tanaka, T. Yamagata, Y. Yamamoto, K. Yonehara, and H. Yoshida, Phys. Rev. Lett. **83**, 690 (1999).

[10] T.D. Ford, J.L. Romero, F.P. Brady, C.M. Castaneda, J.R. Drummond, B. McEachern, D.S. Sorensen, Zin Aung, N.S.P. King, A. Klein, and W.G. Love, Phys. Lett. B **195**, 311 (1987).

[11] C. Bérat, M. Buénerd, J.Y. Hostachy, P. Martin, J. Barrette, B. Berthier, B. Fernandez, A. Miczaïka, A. Villari, H.G. Bohlen, S. Kubono, E. Stiliaris, and W. von Oertzen, Nucl. Phys. **A555**, 455 (1993).

[12] I. Lhenry, Nucl. Phys. **A599**, 245c (1996).

[13] W. von Oertzen, Nucl. Phys. **A482**, 357c (1988).

[14] R.G.T. Zegers, G.P.A. Berg, S. Brandenburg, C.C. Foster, M.N. Harakeh, J. Jänecke, T. O'Donnell, T. Rinckel, D.A. Roberts, S. Shaheen, E.J. Stephenson, and S.Y. van der Werf, Phys. Rev. C **61**, 054602 (2000).

[15] C. Ellegaard, C. Gaarde, J.S. Larsen, C. Goodman, I. Bergqvist, L. Carlén, P. Ekström, B. Jakobsson, J. Lyttkens, M. Bedjidian, M. Chamcham, J.Y. Grossiord, A. Guichard, M. Gusakow, R. Haroutunian, J.R. Pizzi, D. Bachelier, J.L. Boyard, T. Hennino, J.C. Jourdain, M. Roy-Stephan, M. Boivin, and P. Radvanyi, Phys. Rev. Lett. **50**, 1745 (1983).

[16] N. Auerbach, F. Osterfeld, and T. Udagawa, Phys. Lett. B **219**, 184 (1989).

[17] D.L. Prout *et al.*, in *Polarization Phenomena in Nuclear Physics*, edited by E.J. Stephenson and S. Vigdor, AIP Conf. Proc. No. 339 (AIP, Woodbury, NY, 1995), p. 458.
[18] D.L. Prout, J. Rapaport, E. Sugarbaker, D. Cooper, S. Delucia, B. Luther, C.D. Goodman, B.K. Park, L. Rybarcyk, T.N. Taddeucci, and J. Ullmann, Phys. Rev. C **63**, 014603 (2001).
[19] N. Auerbach, Nucl. Phys. **A182**, 247 (1972).
[20] N. Auerbach and A. Yeverechyahu, Ann. Phys. (N.Y.) **95**, 35 (1975).
[21] N. Auerbach and A. Klein, Phys. Rev. C **28**, 2075 (1983).
[22] S. Adachi and N. Auerbach, Phys. Lett. **131B**, 11 (1983).
[23] W.G. Love and M.A. Franey, Phys. Rev. C **24**, 1073 (1981).
[24] F. Osterfeld, Rev. Mod. Phys. **64**, 491 (1992).
[25] R.G.T. Zegers, A.M. van den Berg, S. Brandenburg, F.R.R. Fleurot, M. Fujiwara, J. Guillot, V.M. Hannen, M.N. Harakeh, H. Laurent, K. van der Schaaf, S.Y. van der Werf, A. Willis, and H.W. Wilschut, Phys. Rev. Lett. **84**, 3779 (2000).
[26] N. Matsuoka, A. Shimizu, K. Hosono, T. Saito, M. Kondo, H. Sakaguchi, A. Goto, and F. Ohtani, Nucl. Phys. **A337**, 269 (1980).
[27] E.H.L. Aarts, R.K. Bhowmik, R.J. de Meijer, and S.Y. van der Werf, Phys. Lett. **102B**, 307 (1981).
[28] M.N. Harakeh, H. Akimune, I. Daito, Y. Fujita, M.B. Greenfield, T. Inomata, J. Jänecke, K. Katori, S. Nakayama, H. Sakai, Y. Sakemi, M. Tanaka, and M. Yosoi, Nucl. Phys. **A577**, 57c (1994).
[29] H. Akimune, I. Daito, Y. Fujita, M. Fujiwara, M.B. Greenfield, M.N. Harakeh, T. Inomata, J. Jänecke, K. Katori, S. Nakayama, H. Sakai, Y. Sakemi, M. Tanaka, and M. Yosoi, Phys. Rev. C **52**, 604 (1995).
[30] H. Akimune, I. Daito, Y. Fujita, M. Fujiwara, M.N. Harakeh, J. Jänecke, and M. Yosoi, Phys. Rev. C **61**, 011304(R) (1999).
[31] E.A. Moukhai, V.A. Rodin, and M.H. Urin, Phys. Lett. B **447**, 8 (1999).
[32] M.L. Gorelik, V.A. Rodin, and M.H. Urin, Proceedings of the International Conference on Giant Resonances, Osaka, 2000 (Nucl. Phys. A, to be published).
[33] A.M. van den Berg, Nucl. Instrum. Methods Phys. Res. B **99**, 637 (1995).
[34] E. Plankl-Chabib, Ph.D. thesis, Université Paris XI, Orsay, 1999.
[35] Z. Zojceski, Ph.D. thesis, Université Paris XI, Orsay, 1997.
[36] J.C. Artiges, V. Hervier, A. Richard, P. Volkov, E. Wanlin, and Z. Zojcseski, IEEE Trans. Nucl. Sci. **43**, 1784 (1996).
[37] R.G.T. Zegers, Ph.D. thesis, Rijksuniversiteit Groningen, 1999.
[38] E.N.E. van Dalen, KVI Internal Report No. 205I, 1998.
[39] J.A. Bordewijk, Ph.D. thesis, Rijksuniversiteit Groningen, 1993.
[40] J. Jänecke, K. Pham, D.A. Roberts, D. Stewart, M.N. Harakeh, G.P.A. Berg, C.C. Foster, J.E. Lisantti, R. Sawafta, E.J. Stephenson, A.M. van den Berg, S.Y. van der Werf, S.E. Muraviev, and M.H. Urin, Phys. Rev. C **48**, 2828 (1993).
[41] A. Bohr and B.R. Mottelson, *Nuclear Structure*, (Benjamin, New York, 1975), Vols. 1 and 2.
[42] R. Ö. Akyüz and S. Fallieros, Phys. Rev. Lett. **27**, 1016 (1971).
[43] P. Paul, F. Amann, and K.A. Snover, Phys. Rev. Lett. **27**, 1013 (1971).
[44] B.L. Berman and S.C. Fultz, Rev. Mod. Phys. **47**, 713 (1975).
[45] M.A. Hofstee, S.Y. van der Werf, A.M. van der Berg, N. Blasi, J.A. Bordewijk, W.T.A. Borghols, R. De Leo, G.T. Emery, S. Fortier, S. Galès, M.N. Harakeh, P. den Heijer, C.W. de Jager, H. Langevin-Joliot, S. Micheletti, M. Morlet, M. Pignanelli, J.M. Schippers, H. de Vries, A. Willis, and A. van der Woude, Nucl. Phys. **A588**, 729 (1995).
[46] S.Y. van der Werf, computer code NORMOD, KVI Groningen, 1991 (unpublished).
[47] R. Schaeffer and J. Raynal, computer code DWBA70, SPtH, 1970 (unpublished); J.R. Comfort, extended version DW81, University of Pittsburgh, 1981 (unpublished).
[48] S.Y. van der Werf, Phys. Scr. **T32**, 43 (1990).
[49] J. Jänecke *et al.* (unpublished).
[50] S.L. Tabor, G. Neuschaeffer, J.A. Carr, F. Petrovich, C.C. Chang, A. Guterman, M.T. Collins, D.L. Friesel, C. Glover, S.Y. van der Werf, and S. Raman, Nucl. Phys. **A422**, 12 (1984).
[51] N. Willis, I. Brissaud, Y. le Bornec, B. Tatischeff, and G. Duhamel, Nucl. Phys. **A204**, 454 (1973).
[52] S.Y. van der Werf, S. Brandenburg, P. Grasdijk, W.A. Sterrenburg, M.N. Harakeh, M.B. Greenfield, B.A. Brown, and M. Fujiwara, Nucl. Phys. **A496**, 305 (1989).
[53] V.A. Kuzmin and V.G. Soloviev, J. Phys. G **11**, 603 (1985).
[54] C. Gaarde, J.S. Larsen, A.G. Drentje, M.N. Harakeh, and S.Y. van der Werf, Phys. Rev. Lett. **46**, 902 (1981).
[55] W.T.A. Borghols, Ph.D. thesis, Rijksuniversiteit Groningen, 1988.
[56] C. Sükösd, C. Mayer-Böricke, M. Rogge, P. Turek, K.T. Knöpfle, H. Riedesel, K. Schindler, and G.J. Wagner, Nucl. Phys. **A467**, 365 (1987).
[57] F. Pühlhofer, Nucl. Phys. **A280**, 267 (1977); computer code CASCADE, 1979 (unpublished); M.N. Harakeh, extended version, 1983 (unpublished).
[58] C. Gaarde, J. Rapaport, T.N. Taddeucci, C.D. Goodman, C.C. Foster, D.E. Bainum, C.A. Goulding, M.B. Greenfield, D.J. Horen, and E. Sugarbaker, Nucl. Phys. **A369**, 258 (1981).
[59] K. Shimizu, M. Ichimura, and A. Arima, Nucl. Phys. **A226**, 282 (1974).
[60] H. Hyuga, A. Arima, and K. Shimizu, Nucl. Phys. **A336**, 363 (1980).
[61] A. Arima, Nucl. Phys. **A649**, 260c (1999).
[62] M. Ericson, A. Figureau, and C. Thévenet, Phys. Lett. **45B**, 19 (1973).